Pergamon

*Int. J. Solids Structures* Vol. 33, No. 19, pp. 2775–2787, 1996

0020–7683/96 $15.00 + .00

0020–7683(95)00180–8

# DIRECT IDENTIFICATION OF NON-UNIFORM BEAMS USING STATIC STRAINS

PEI-LING LIU and HWEI-TSER LIN
Institute of Applied Mechanics, National Taiwan University, Taipei, Taiwan, R.O.C.

(*Received* 1 *June* 1994; *in revised form* 20 *July* 1995)

**Abstract**—A method for identifying the flexural rigidities of a non-uniform beam is developed in this paper. The finite element method is used to derive the equilibrium equation of the beam. The identification problem is then formulated as an optimization program in which the error norm of the equilibrium equation is minimized. The proposed method has the following features: (1) it uses longitudinal strains as the primary test data; (2) the solution is unique and global minimal; (3) the method can be applied to a whole beam as well as a part of a beam; (4) the method is very stable. The identifiability of the inverse problem is studied in depth. Two numerical examples are presented to demonstrate the proposed method. Finally, a model test is performed to examine the effectiveness of the method in real applications. Copyright © 1996 Elsevier Science Ltd.

## 1. INTRODUCTION

The use of identification techniques to determine the properties of a structure has been attempted recently. Several studies (Yun and Shinozuka, 1980; Shinozuka *et al.*, 1982; Hoshiya and Saito, 1984; Lin *et al.*, 1990; Agbabian *et al.*, 1991; Hoshiya and Maruyama, 1991) have used the response of a structure measured in a dynamic test to identify the dynamic system. Either the least-squares method or the extended Kalman filter has been proposed in these studies.

In addition to the aforementioned approaches, Baruch and Bar-Itzhack (1978), Berman and Nagy (1983), Kabe (1985), Kammer (1987), Chen and Garba (1988), and Smith and Beattie (1991) have adopted modal data to identify the global stiffness and/or mass matrices of a structure. The problem has been formulated as an optimization program in which the deviation of the current stiffness matrix from the original stiffness matrix is minimized. Some of these approaches also include constraints to retain the symmetry and sparsity of the stiffness matrix. Liu (1995) has incorporated the finite-element formulation in the least-squares inversion to determine the axial rigidities of a truss using modal data.

Sanayei and Onipede (1991), Sanayei and Scampoli (1991), and Hajela and Soeiro (1990) have suggested that static test data (displacements) be used in association with the least-squares method to compute the stiffness at element level. Their error functions are in terms of the difference between the measured and analytical nodal displacements. Since structural response can be measured precisely in a static test, these methods are expected to yield reliable results. Furthermore, it is easy to detect the damage locations from the identification results since the stiffness parameter is attained for each element.

The inverse method developed in this study employs the finite element method together with the least-squares method to solve for the flexural rigidity of a beam. Instead of nodal displacements and rotations, the proposed method utilizes the longitudinal strains of the beam measured in static tests as the input data. The use of such data has the advantage that the element strains can be easily measured by strain gages during the tests. If the nodal displacements and rotations are used instead, more complicated or costly experimental set-up would be needed to measure such quantities. Hence, the strain formulation is expected to be more feasible in practice. The details are given in the following sections.

## 2. FINITE ELEMENT FORMULATION

The behavior of a non-uniform beam in a static test can be predicted by the finite element method. Suppose the beam is discretized into $m$ elements, and the flexural rigidity in each element is assumed to be constant. The equilibrium equation of a beam element can be written as

$$\mathbf{k}_e\mathbf{u}_e = \mathbf{f}_e \tag{1}$$

where $\mathbf{k}_e$ is the stiffness matrix, and $\mathbf{f}_e$ is the force vector of the element, respectively; $\mathbf{u}_e = [w_1, \varphi_1, w_2, \varphi_2]^T$ contains the nodal displacements and rotations at the two nodes (see Fig. 1). If the conventional beam element is adopted, $\mathbf{k}_e = EI_e\mathbf{A}_e$, where $EI_e$ is the flexural rigidity of the element, and

$$\mathbf{A}_e = \begin{bmatrix} \frac{12}{h^3} & \frac{-6}{h^2} & \frac{-12}{h^3} & \frac{-6}{h^2} \\ \frac{-6}{h^2} & \frac{4}{h} & \frac{6}{h^2} & \frac{2}{h} \\ \frac{-12}{h^3} & \frac{6}{h^2} & \frac{12}{h^3} & \frac{6}{h^2} \\ \frac{-6}{h^2} & \frac{2}{h} & \frac{6}{h^2} & \frac{4}{h} \end{bmatrix} \tag{2}$$

in which $h$ is the length of the element.

Assembling the element equations and applying the boundary conditions, one can obtain the following equilibrium equation:

$$\mathbf{KU} = \mathbf{F} \tag{3}$$

where $\mathbf{K}$, $\mathbf{U}$, and $\mathbf{F}$ are the global stiffness matrix, nodal displacement vector, and nodal force vector of the beam, respectively.

In forward calculations, the unknown displacements can be obtained by solving eqn (3) directly. In inverse problems, the purpose is to compute the flexural rigidities of the elements using the response measured in structural tests. In that case, the displacement vector $\mathbf{U}$ is known, while $\mathbf{K}$ is not since it depends on the unknown rigidities $EI_e$. Hence, it is useful to rewrite eqn (3) so that $\mathbf{S} = [EI_1, EI_2, \ldots, EI_m]^T$ appears explicitly in the equation.

The global stiffness matrix can be written as

$$\mathbf{K} = \sum_{e=1}^{m} \mathbf{K}_e = \sum_{e=1}^{m} EI_e\mathbf{L}_e\mathbf{A}_e\mathbf{L}_e^T \tag{4}$$

where $\mathbf{L}_e$ is an $n \times 4$ connectivity matrix that links the local DOFs to the global DOFs,

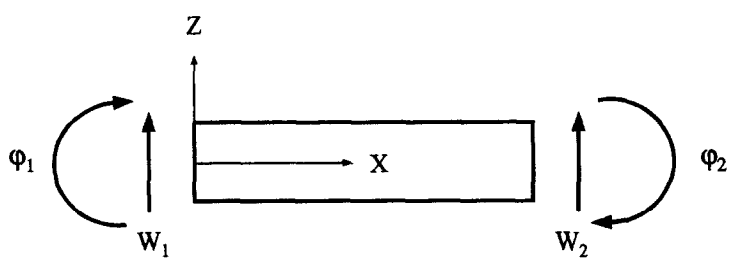


Fig. 1. Beam element.

where $n$ is the number of DOFs of the beam. Obviously, $\mathbf{L}_e$ and $\mathbf{A}_e$ are independent of the unknown properties $EI_e$. It follows that

$$\mathbf{KU} = \sum_{e=1}^{m} EI_e \mathbf{L}_e \mathbf{A}_e \mathbf{L}_e^{\mathrm{T}} \mathbf{U} = \mathbf{PS} \tag{5}$$

where

$$\mathbf{P} = [\mathbf{L}_1 \mathbf{A}_1 \mathbf{L}_1^{\mathrm{T}} \mathbf{U}, \ldots, \mathbf{L}_m \mathbf{A}_m \mathbf{L}_m^{\mathrm{T}} \mathbf{U}]. \tag{6}$$

Finally, the equilibrium equation can be rewritten as

$$\mathbf{PS} = \mathbf{F}. \tag{7}$$

Notice that each column of $\mathbf{P}$ multiplied by its corresponding $EI_e$ is equal to the resisting force vector of the element.

## 3. INVERSION OF ELEMENT RIGIDITIES

Suppose $\mathscr{K}$ static tests are performed on a target beam. Identification of the beam properties can be formulated as the following optimization problem:

$$\begin{aligned} &\text{minimize} \quad \mathscr{E} = \sum_{k=1}^{\mathscr{K}} |\mathbf{P}_k \mathbf{S} - \mathbf{F}_k|^2 \\ &\text{subject to} \quad \mathbf{S} \geqslant \mathbf{0} \end{aligned} \tag{8}$$

where $\mathscr{E}$ is the error function, and the subscript $k$ denotes the test number. The error function is a non-negative function. In the ideal case, its value approaches zero when the rigidity of the beam elements are exact.

Such formulation has two advantages over the widely used output-error approach in which the difference between the computed and measured data is minimized. First of all, no solution of the equilibrium equation is necessary in this equation-error formulation. Secondly, $\mathscr{E}$ is a purely quadratic function in $\mathbf{S}$. Hence, this formulation has a unique solution.

In the absence of the constraints $\mathbf{S} \geqslant \mathbf{0}$, the minimal value of $\mathscr{E}$ can be obtained directly by setting $\partial \mathscr{E}/\partial \mathbf{S}$ to zero. It follows that

$$\sum_{k=1}^{\mathscr{K}} \mathbf{P}_k^{\mathrm{T}} \mathbf{P}_k \mathbf{S} = \sum_{k=1}^{\mathscr{K}} \mathbf{P}_k^{\mathrm{T}} \mathbf{F}_k. \tag{9}$$

In short, it can be written as

$$\mathbf{HS} = \mathbf{R}. \tag{10}$$

If the coefficient matrix $\mathbf{H}$ is non-singular, this equation can be solved for $\mathbf{S}$ directly.

In most cases, the solution of eqn (10) also satisfies the set constraints $\mathbf{S} \geqslant \mathbf{0}$. Then, it is also the solution of the inverse problem in eqn (8). However, when there are errors in the data, it is possible that some elements of $\mathbf{S}$ are negative. Evidently, that is not a feasible solution of eqn (8).

The problem of unfeasibility can be tackled using the active set method (Luenberger, 1984). To apply the active set method, one has to find a feasible point to begin with. Let $\mathbf{S}^*$ denote the solution of eqn (10). Partition $\mathbf{S}^*$ into two subvectors $\mathbf{S}_1^*$ and $\mathbf{S}_2^*$ such that $\mathbf{S}_1^* \leqslant 0$ and $\mathbf{S}_2^* > 0$. Let $k = 0$ and

$$\mathbf{S}^0 = \begin{bmatrix} \mathbf{0} \\ \mathbf{S}_2^* \end{bmatrix} \tag{11}$$

where the superscript 0 denotes the zeroth iteration. Then, $\mathbf{S}_1 \geqslant \mathbf{0}$ are the active constraints, and $\mathbf{S}_2 \geqslant \mathbf{0}$ are the inactive constraints in the first step.

The minimum point of eqn (8) can be found by the following iteration:

(1) Solve the quadratic program:

$$\begin{aligned} &\text{minimize} \quad \mathscr{E}(\mathbf{S}) \\ &\text{subject to} \quad \mathbf{S}_1 = \mathbf{0}. \end{aligned} \tag{12}$$

The solution $\bar{\mathbf{S}}$ can be obtained by setting $\partial \mathscr{E}(\mathbf{S}_1 = \mathbf{0}, \mathbf{S}_2)/\partial \mathbf{S}_2$ to zero. No iterations are necessary.

(2) If $\bar{\mathbf{S}}_2$ violates some of the inactive constraints, these constraints are added to the active set, and $\mathbf{S}^{(k+1)}$ is obtained as follows:

$$\mathbf{S}^{(k+1)} = (1-\alpha)\mathbf{S}^k + \alpha \bar{\mathbf{S}} \tag{13}$$

where $\alpha$ is chosen to be the maximum value in (0, 1) such that $\mathbf{S}^{(k+1)} \geqslant 0$. Then, repeat the iteration with the new active set.

(3) Suppose $\bar{\mathbf{S}}$ satisfies $\bar{\mathbf{S}} \geqslant \mathbf{0}$. Then, $\bar{\mathbf{S}}$ should satisfy the first-order necessary conditions

$$\nabla \mathscr{E}(\mathbf{S}) - \begin{bmatrix} \boldsymbol{\lambda}_1 \\ \mathbf{0} \end{bmatrix} = \mathbf{0} \tag{14}$$

where $\boldsymbol{\lambda}_1$ contains the Lagrange multipliers corresponding to the constraints $\mathbf{S}_1 \geqslant 0$.

(a) If $\boldsymbol{\lambda}_1 \geqslant \mathbf{0}$, $\bar{\mathbf{S}}$ is the solution of the inverse problem.

(b) If some of the multipliers are negative, then the objective can be reduced by relaxing the associated constraints. Hence, these constraints should be deleted from the active set. Then, set $\mathbf{S}^{(k+1)} = \bar{\mathbf{S}}$ and repeat the iteration with the new active set.

If the Hessian matrix $\mathbf{H}$ is positive definite, $\mathscr{E}$ is a strictly convex function. According to the active set theorem (Luenberger, 1984), the iterations will converge to the global minimum point in a finite number of steps. In fact, one can easily show that $\mathbf{H}$ is positive semi-definite. Furthermore, $\mathbf{H}$ can be made non-singular, as will be discussed later. Therefore, solution of the inverse problem is guaranteed.

## 4. STRAIN FORMULATION

Although the above solution procedure is rather simple, it is not easy to carry out in practice. The difficulties lie in the measurement of displacements and rotations of a beam in the test. The approach will become more practical if one can express $\mathbf{P}_k$ in terms of the longitudinal strains of the beam because such quantities are routine measurements in structural tests.

In the finite element model, the transverse displacement in an element can be obtained by the following interpolation:

$$w = \mathbf{N}\mathbf{u}_e \tag{15}$$

where $\mathbf{N}$ is a $1 \times 4$ vector containing the four interpolation functions. Hence, the longitudinal strain $\varepsilon$ in the element can be expressed as follows:

$$\varepsilon(x,z) = -\frac{\partial^2 w}{\partial x^2} z$$

$$= -\frac{\partial^2 \mathbf{N}}{\partial x^2} \mathbf{u}_e z$$

$$= \frac{2}{h^2}\left[3-6\frac{x}{h},\quad 3x-2h,\quad 6\frac{x}{h}-3,\quad 3x-h\right]\mathbf{u}_e z$$

$$= \mathbf{c}_e \mathbf{u}_e z \tag{16}$$

where $z$ is the distance from the strain gage to the neutral axis of the cross-section (see Fig. 1). It can be derived that

$$\mathbf{c}_e = \mathbf{a}_{e1} x + \mathbf{a}_{e2} \tag{17}$$

where $\mathbf{a}_{e1}$ and $\mathbf{a}_{e2}$ are the first and second rows of $\mathbf{A}_e$.

Suppose two strain gages are mounted on the element at $(x_1, z_1)$ and $(x_2, z_2)$, respectively. Denote the vector $\mathbf{c}_e$ as $\mathbf{c}_{e1}$ and $\mathbf{c}_{e2}$, respectively, at these locations. Then, using eqn (17), one can express $\mathbf{a}_{e1}$ and $\mathbf{a}_{e2}$ in terms of $\mathbf{c}_{e1}$ and $\mathbf{c}_{e2}$. Consequently, $\mathbf{A}_e$ can be expressed as follows:

$$\mathbf{A}_e = \frac{1}{x_2 - x_1}\begin{bmatrix} \mathbf{c}_{e1} - \mathbf{c}_{e2} \\ -x_2\mathbf{c}_{e1} + x_1\mathbf{c}_{e2} \\ -\mathbf{c}_{e1} + \mathbf{c}_{e2} \\ -(h-x_2)\mathbf{c}_{e1} + (h-x_1)\mathbf{c}_{e2} \end{bmatrix}. \tag{18}$$

Notice that the two gages cannot be mounted on the neutral axis of the beam, i.e. $z = 0$, or on the same cross-section of the beam, i.e. $x_1 = x_2$, otherwise the above expression does not hold.

Recall that the $e$th column of $\mathbf{P}_k$ is $\mathbf{L}_e\mathbf{A}_e\mathbf{L}_e^{\mathrm{T}}\mathbf{U}$. $\mathbf{L}_e^{\mathrm{T}}\mathbf{U}$ is simply the nodal displacement vector $\mathbf{u}_e$. Hence, using eqn (18), one obtains

$$\mathbf{L}_e\mathbf{A}_e\mathbf{L}_e^{\mathrm{T}}\mathbf{U} = \frac{\mathbf{L}_e}{x_2 - x_1}\begin{bmatrix} \dfrac{\varepsilon_1}{z_1} - \dfrac{\varepsilon_2}{z_2} \\ -\dfrac{x_2\varepsilon_1}{z_1} + \dfrac{x_1\varepsilon_2}{z_2} \\ -\dfrac{\varepsilon_1}{z_1} + \dfrac{\varepsilon_2}{z_2} \\ -\dfrac{(h-x_2)\varepsilon_1}{z_1} + \dfrac{(h-x_1)\varepsilon_2}{z_2} \end{bmatrix}. \tag{19}$$

Now, each column of $\mathbf{P}_k$ is expressed in terms of the strains $\varepsilon_1$ and $\varepsilon_2$ and the gage locations $(x_1, z_1)$ and $(x_2, z_2)$. Therefore, one can use the strain measurements to compute $\mathbf{P}_k$ directly. Then, the inversion of $EI_e$ may proceed as discussed previously.

## 5. LOCAL IDENTIFICATION

There are situations in which identification of a whole beam is not suitable, for instance, when the beam is damaged and one only wants to assess the element stiffness near the damaged location. The proposed identification method can be modified to do local identification.

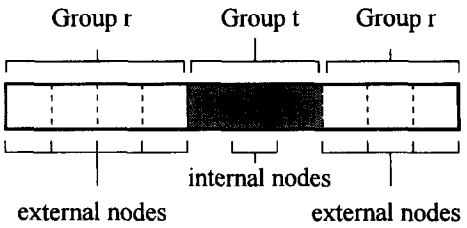


Fig. 2. Beam partition for local identification.

First of all, divide the beam elements into two groups: Group $t$ comprises the target elements to be identified, and Group $r$ comprises the remaining elements (see Fig. 2). Then, the nodes only connected to Group $t$ elements are called internal nodes, and the remaining nodes are called external nodes. According to such partition, the equilibrium at the internal nodes can be stated as follows:

$$\mathbf{P}^{it}\mathbf{S}^t = \mathbf{F}^i \tag{20}$$

where $\mathbf{P}^{it}$ is a submatrix of $\mathbf{P}$, the superscript $i$ denotes the rows corresponding to the internal nodes, and $t$ denotes the columns corresponding to Group $t$ elements. Similar to $\mathbf{P}$, each column of $\mathbf{P}^{it}$ multiplied by its corresponding $EI_e$ gives the resisting forces of the element at the internal nodes.

To perform local identification, the strains of all the target elements must be measured. Once the strains of the Group $t$ elements are known, one can use eqn (19) to construct the resisting force vectors of these elements. Then, removing the rows corresponding to the external nodes from these vectors yields $\mathbf{P}^{it}$.

Hence, local identification of the beam can be formulated as the following optimization problem:

$$\text{minimize} \quad \mathscr{E}_\ell = \sum_{k=1}^{\mathscr{K}} |\mathbf{P}_k^{it}\mathbf{S}^t - \mathbf{F}_k^i|^2 \tag{21}$$

$$\text{subject to} \quad \mathbf{S}^t \geqslant \mathbf{0}$$

where $\mathscr{E}_\ell$ is the new error function for the local identification. Different from eqn (8), this error function is in terms of the residual forces at the internal nodes, not all nodes. Therefore, the loads must be applied at the internal nodes. Otherwise, $\mathbf{F}_k^i = \mathbf{0}$, and one only arrives at the trivial solution.

This optimization program has exactly the same structure as that in eqn (8). Hence, the solution procedure is identical to that of total identification except that $\mathbf{P}_k$, $\mathbf{S}$, and $\mathbf{F}_k$ should be replaced by $\mathbf{P}_k^{it}, \mathbf{S}^t$, and $\mathbf{F}_k^i$, respectively. The solution also possesses the nice properties of being unique and globally minimal.

Undoubtedly, one may use the above method for the identification of a whole beam simply by including all elements in Group $t$. In that case, the two end nodes of the beam are external nodes. Hence, force equilibrium at these nodes does not appear in the error function. This is equivalent to total identification of the beam while keeping the two ends clamped. Therefore, identification of a beam can be carried out regardless of the boundary conditions of the beam. Needless to say, that is a very nice feature because the beam is unlikely to be perfectly clamped or hinged in reality.

## 6. IDENTIFIABILITY

The inverse problem has a unique solution as long as the Hessian matrix of $\mathscr{E}$ is non-singular. Therefore, the rank of $\mathbf{H}$ will be examined in this section.

Recall that $\mathbf{H} = \sum_{k=1}^{\mathscr{K}} \mathbf{P}_k^{\mathrm{T}}\mathbf{P}_k$. Firstly, let us consider only one test. Since $\mathrm{rank}(\mathbf{P}_1^{\mathrm{T}}\mathbf{P}_1) = \mathrm{rank}(\mathbf{P}_1)$, we may evaluate the rank of $\mathbf{P}_1$ instead of its product. Notice that

$\mathbf{P}_1$ is an $n \times m$ matrix, and each column of $\mathbf{P}_1$ is equal to $\mathbf{L}_e\mathbf{A}_e\mathbf{L}_e^{\mathrm{T}}\mathbf{U}_1$. Take a cantilever beam for example,

$$\mathbf{P}_1 = \begin{bmatrix} \mathbf{a}_{13}\mathbf{u}_1 & \mathbf{a}_{21}\mathbf{u}_2 & 0 & \cdot & \cdot & 0 \\ \mathbf{a}_{14}\mathbf{u}_1 & \mathbf{a}_{22}\mathbf{u}_2 & 0 & \cdot & \cdot & 0 \\ 0 & \mathbf{a}_{23}\mathbf{u}_2 & \mathbf{a}_{31}\mathbf{u}_3 & \cdot & \cdot & 0 \\ 0 & \mathbf{a}_{24}\mathbf{u}_2 & \mathbf{a}_{32}\mathbf{u}_3 & \cdot & \cdot & 0 \\ \cdot & \cdot & \cdot & \cdot & \cdot & \cdot \\ 0 & 0 & \cdot & \cdot & \mathbf{a}_{(m-1)3}\mathbf{u}_{m-1} & \mathbf{a}_{m1}\mathbf{u}_m \\ 0 & 0 & \cdot & \cdot & \mathbf{a}_{(m-1)4}\mathbf{u}_{m-1} & \mathbf{a}_{m2}\mathbf{u}_m \\ 0 & 0 & \cdot & \cdot & 0 & \mathbf{a}_{m3}\mathbf{u}_m \\ 0 & 0 & \cdot & \cdot & 0 & \mathbf{a}_{m4}\mathbf{u}_m \end{bmatrix} \tag{22}$$

where $\mathbf{a}_{ei}$ is the $i$th row of $\mathbf{A}_e$, and $\mathbf{u}_e$ is the displacement vector of element $e$. The first column of $\mathbf{P}_1$ has only two non-zero elements because the first two DOFs of the first element are fixed.

Suppose there are $q$ zero columns in $\mathbf{P}_1$. One can easily show that $\mathrm{rank}(\mathbf{P}_1) = m-q$ using the definition of linear dependence. As mentioned before, the gage locations must be such that $x_1 \neq x_2$. Hence, the columns of $\mathbf{P}_1$ do not vanish unless $\varepsilon_1 = \varepsilon_2 = 0$. If the load is applied at the free end of the cantilever beam, $\varepsilon$ does not vanish anywhere. It follows that $\mathrm{rank}(\mathbf{P}_1) = m$.

If the beam is clamped at both ends, $\mathbf{P}_1$ becomes

$$\mathbf{P}_1 = \begin{bmatrix} \mathbf{a}_{13}\mathbf{u}_1 & \mathbf{a}_{21}\mathbf{u}_2 & 0 & \cdot & \cdot & 0 \\ \mathbf{a}_{14}\mathbf{u}_1 & \mathbf{a}_{22}\mathbf{u}_2 & 0 & \cdot & \cdot & 0 \\ 0 & \mathbf{a}_{23}\mathbf{u}_2 & \mathbf{a}_{31}\mathbf{u}_3 & \cdot & \cdot & 0 \\ 0 & \mathbf{a}_{24}\mathbf{u}_2 & \mathbf{a}_{32}\mathbf{u}_3 & \cdot & \cdot & 0 \\ \cdot & \cdot & \cdot & \cdot & \cdot & \cdot \\ 0 & 0 & \cdot & \cdot & \mathbf{a}_{(m-1)3}\mathbf{u}_{m-1} & \mathbf{a}_{m1}\mathbf{u}_m \\ 0 & 0 & \cdot & \cdot & \mathbf{a}_{(m-1)4}\mathbf{u}_{m-1} & \mathbf{a}_{m2}\mathbf{u}_m \end{bmatrix}. \tag{23}$$

Suppose there are $q$ zero columns in the first $(m-1)$ columns of $\mathbf{P}_1$. It is easy to show that there are $(m-1-q)$ independent vectors in these columns. The last column is a linear combination of the remaining columns if

$$\begin{bmatrix} \mathbf{a}_{e3}\mathbf{u}_e \\ \mathbf{a}_{e4}\mathbf{u}_e \end{bmatrix} \propto \begin{bmatrix} \mathbf{a}_{(e+1)1}\mathbf{u}_{e+1} \\ \mathbf{a}_{(e+1)2}\mathbf{u}_{e+1} \end{bmatrix} \quad e = 1, 2, \ldots, m-1. \tag{24}$$

Therefore, $\mathbf{P}_1$ is either of rank $(m-1-q)$ or $(m-q)$ depending on whether eqn (24) is satisfied or not. One can show that eqn (24) will never hold if the beam elements have equal lengths. In that case, $\mathbf{P}_1$ is of rank $(m-q)$.

The rank of $\mathbf{P}_1$ can be derived in a similar way for beams with other boundary conditions. The only difference is that the form of $\mathbf{P}_1$ will change because only the rows corresponding to the free DOFs appear in $\mathbf{P}_1$.

From the above discussions, it can be concluded that $\mathrm{rank}(\mathbf{H})$ does not exceed $(m-q)$ if only one set of test data is considered. Since $\mathbf{H}$ is a $m \times m$ matrix, it is possible that $\mathbf{H}$ is singular if only one set of test data are used.

The problem of singularity can be resolved by including more test data. Take a clamped–clamped beam for example. Suppose the $i$th column of $\mathbf{P}_1$ is a zero vector and does not contribute to the rank of $\mathbf{P}_1$. If a second test is performed,

$$\text{rank}(\mathbf{H}) = \text{rank}\begin{bmatrix}\mathbf{P}_1\\ \mathbf{P}_2\end{bmatrix}. \tag{25}$$

By the definition of linear dependence, one can show that if $\varepsilon_1$ and $\varepsilon_2$ of the $i$th element do not vanish identically in the second test, the rank of $\mathbf{H}$ will be increased by one. On the other hand, if eqn (24) holds and rank $(\mathbf{P}_1) = (m-1-q)$, one can apply a different set of loading in the second test so that the last column of $\mathbf{P}_2$ is independent of the first $(m-1)$ columns. Following the above procedure, $\mathbf{H}$ will eventually become non-singular when all the zero and dependent columns in $\mathbf{P}_1$ have been dealt with.

In practice, it may be difficult for engineers to follow the procedure presented in this section. Therefore, some useful guidelines are provided in the following.

(1) Cantilever beam
Apply a load at the free end of the beam.
(2) Simply-supported beam
Apply a load around the mid-span of the beam.
(3) Clamped–hinged beam
Apply a load around the mid-span of the beam. For the element connected to the hinged end, mount the gages such that $z_1 = z_2$ or $z_1 z_2 < 0$.
(4) Clamped–clamped beam
Apply a load around the mid-span of the beam. Discretize the beam such that the lengths of the two elements next to the loads are equal.

In the above, the load can be either a concentrated force or a moment. Following these guidelines, a single set of test data would yield a non-singular $\mathbf{H}$. Notice that three out of the four guidelines suggest that the load be applied near the mid-span. This is not due to the identifiability concern but the accuracy concern. If the load is applied next to the clamped end, the beam hardly deforms, and one cannot expect to attain reliable results.

It has just been shown that if the tests are properly designed, the inverse problem has a unique solution. However, care must be taken when the strain formulation is adopted, especially when unexpected change may occur in the beam rigidity. Take a uniform cantilever beam for example. Suppose a cut is made in the beam, and the flexural rigidity is reduced at that section. If the strain gages are not mounted right on the cut section, the strain readings would be exactly the same as if the beam were uniform. In that case, one cannot detect the change of the beam rigidity.

The most straightforward solution to this problem is to mount as many gages as possible, especially at sections where the rigidity may change abruptly. Another solution is to employ the displacement formulation instead because the displacements and rotations are dependent on the rigidity distribution of the whole beam. If it is difficult to measure the displacements and rotations at all nodes, one may make measurement at a few properly selected nodes. Then, either add $\Sigma_i(\mathbf{U}_i - \bar{\mathbf{U}}_i)^2$ to the error function as a penalty term or add $\mathbf{U}_i = \bar{\mathbf{U}}_i$ to the optimization program as constraints, where $\mathbf{U}_i$ and $\bar{\mathbf{U}}_i$ are the computed and measured displacements and/or rotations at these nodes, respectively. Hopefully, this would force the optimization problem to yield accurate results.

## 7. NUMERICAL EXAMPLES

### 7.1. *Tapered beam identification*

Consider a tapered beam which is made of aluminum with Young's modulus 70 Gpa. The beam is 400 mm in length and has a constant thickness of 12 mm. The width of the beam decreases linearly from 25 mm at the left end to 20 mm at the right end. Hence, the flexural rigidity of the beam varies linearly from 252 N m$^2$ at the left end to 201.6 N m$^2$ at the right end. The beam is discretized into 10 elements of equal length, 40 mm. Two strain gages are mounted on the bottom of each element at $x_1 = 10$ mm and $x_2 = 30$ mm, respectively.

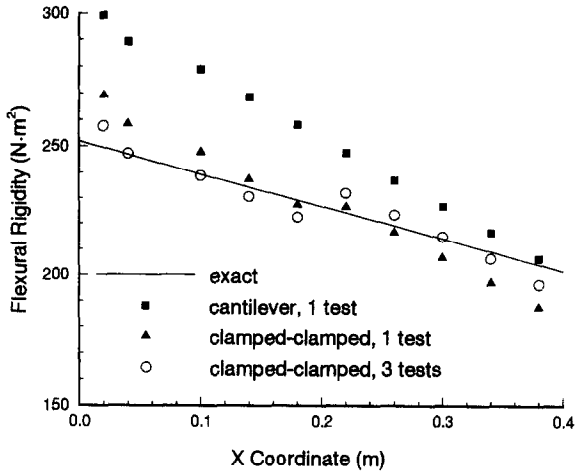


Fig. 3. Results of tapered beam identification.

Firstly, consider the beam to be clamped at the left end. According to the previous discussions, the rank of **P** is equal to 10 in this case. Since there are 10 unknowns, only one set of test data is required to yield a non-singular **H** if the load is applied at the free end. Hence, integration was carried out to compute the element strains due to a vertical load of 200 N(↓) at the free end of the beam. Notice that the analytical solution and the finite element solution are not identical in this case since in the finite element model the beam cross-section is uniform in each element, not tapered.

The results were then used as input data to identify the flexural rigidities of the beam elements. The identification was carried out on a DEC 3000 Model 400 AXP workstation, and the job took only 0.08s of CPU time (approximately 0.5s on a 486DX personal computer). The identified rigidities are shown in Fig. 3. It is seen that the trend of the flexural rigidity can be recovered successfully, but the maximum error is 18.8%. The errors certainly arise from the discrepancy between the analytical model and the finite element model.

The analysis was repeated for the beam with two ends clamped and a load of 200 N(↓) applied at the mid-span. The results are also shown in Fig. 3. It is seen that when extra constraints are imposed on the beam, the maximum error is reduced to 8.0%.

The same strain readings were employed to do local identification for elements 3–7 of the beam. The same results were obtained as in total identification.

In order to investigate the influence of loading conditions, additional tests were carried out. In each test, a 200 N(↓) load was applied at a different nodal point. Figure 4 shows the variation of the maximum error as the load moves. It is seen that the case with the load

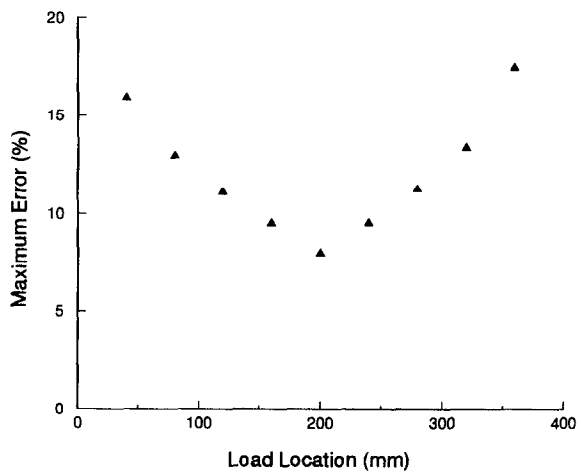


Fig. 4. Influence of load location.

Table 1. Identification results under various loading conditions

| Element number | 200 N at 80 mm $EI$ (N m$^2$) | Error (%) | 200 N at 200 mm $EI$ (N m$^2$) | Error (%) | 200 N at 320 mm $EI$ (N m$^2$) | Error (%) |
|---|---|---|---|---|---|---|
| 1 | 256.54 | 2.83 | 269.15 | 7.88 | 282.81 | 13.36 |
| 2 | 246.28 | 0.75 | 258.43 | 5.72 | 271.59 | 11.11 |
| 3 | 243.85 | 1.86 | 247.89 | 3.55 | 260.54 | 8.83 |
| 4 | 233.96 | −0.17 | 237.57 | 1.37 | 249.69 | 6.54 |
| 5 | 224.16 | −2.25 | 227.49 | −0.80 | 239.08 | 4.26 |
| 6 | 214.48 | −4.37 | 226.72 | 1.09 | 228.74 | 1.99 |
| 7 | 204.96 | −6.51 | 216.68 | −1.17 | 218.69 | −0.25 |
| 8 | 195.64 | −8.66 | 206.84 | −3.44 | 208.96 | −2.45 |
| 9 | 186.55 | −10.81 | 197.22 | −5.71 | 207.70 | −0.70 |
| 10 | 177.72 | −12.94 | 187.85 | −7.97 | 197.81 | −3.09 |

applied at the mid-span yields the best results. Furthermore, the maximum error increases as the load moves towards the ends of the beam. Therefore, it is advisable to apply the load as close to the mid-span as possible.

Table 1 lists the identification results for three loading conditions, the load being applied at 80 mm, 200 mm, and 320 mm from the left end of the beam, respectively. Obviously, the error grows as the distance between the element and the load increases. The same conclusion can also be drawn for the cantilever beam, as shown in Fig. 3. Notice that all components of **R** in eqn (10) vanish except two. These non-zero components correspond to the elements connected to the loading node. This attribute may be the cause for the error increase.

The identification results can be improved by performing more tests. In general, the loading points in the tests should range across the beam span so that all the elements can be identified accurately. If the strain readings of all the three tests in Table 1 are used as input, the maximum error is reduced to 3.7% (see Fig. 3).

Finally, the influence of noise level was investigated. Random noise of various levels was superposed to the element strains of the clamped–clamped, 3-test case. A thousand Monte Carlo simulations were performed for each noise level, and the statistics of the identified rigidities were computed. Figure 5 shows the coefficients of variation of $EI_1$ and $EI_{10}$ under various noise level. The highest noise level considered is $10^{-5}$, which is of the same order as most of the strain readings in the three tests. It is seen that the coefficients of variation increase linearly with the magnitude of the noise. The coefficients of variation of other rigidities have similar behavior. Obviously, the identification method is stable.

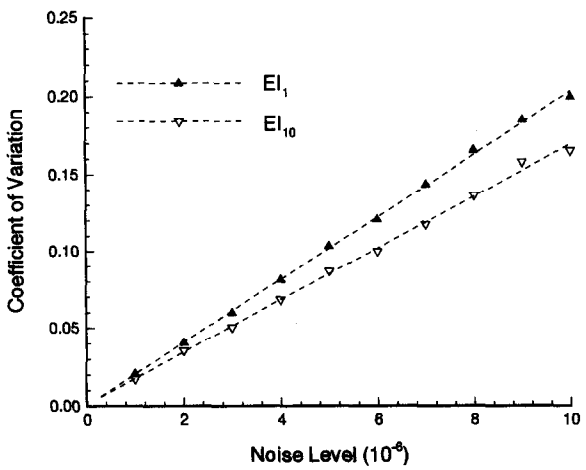


Fig. 5. Influence of noise level.

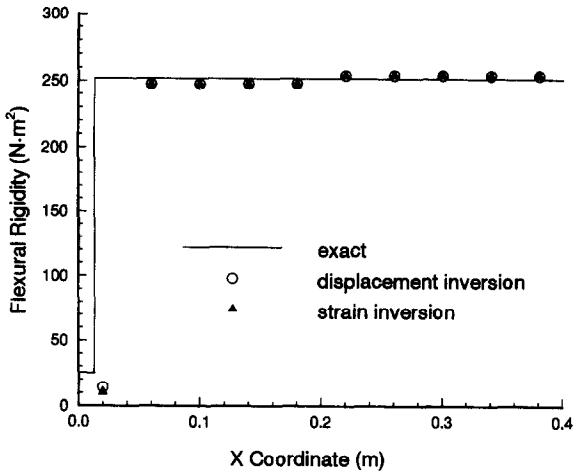


Fig. 6. Results of damaged beam identification.

*7.2. Damaged beam identification*

Consider a uniform beam with both ends clamped. The material and length of the beam are the same as the tapered beam, so are the locations of the strain gages. The cross-section of the beam is 25 mm($W$) × 12 mm($H$). Hence, the flexural rigidity of the beam is originally 252 N m$^2$ throughout the beam.

Suppose 1/30 of the beam span is damaged at the left end of the beam, and the flexural rigidity of the damaged section is reduced to 25.2 N m$^2$ (see Fig. 6). Finite element analysis was carried out to compute the response of the beam using a uniform mesh of 30 elements. In this case, the finite element solution is the same as the analytical solution.

Firstly, identification was carried out using a uniform mesh of 30 elements. Because no noise exists and the same model was adopted in the forward solution as well as in the identification, exact solution was obtained, as expected.

In real applications, the damaged locations are not exactly known. Hence, it is more likely that the damage section does not span a whole element. To simulate such situation, identification was carried out again using a finite element mesh of only 10 elements. In that case, only one-third of the first element was damaged. Because the gages were mounted on $x_1 = 10$ mm and $x_2 = 30$ mm locations, only the first gage measured the strain at a damaged section.

Both the strain and displacement inversions were carried out. These two approaches gave close results, as shown in Fig. 6. Apparently, the damage was detected successfully. The element rigidities were also recovered accurately except at the damaged element. If more accurate results are needed at the damaged location, one may refine the mesh at that location and repeat the identification process.

## 8. MODEL TEST

A model test was carried out to examine the effectiveness of the proposed method in practical applications. The model is a 400 mm long cantilever beam. It is made of aluminum with Young's modulus 61.78 GPa. The cross-section is 25.5 mm($W$) × 9.5 mm($H$) throughout the beam. Thus, the flexural rigidity of beam is 112.6 N m$^2$. At the free end, the beam has a 70 mm extension at which loads can be applied.

The beam was discretized into 4 elements, 100 mm long each. Two TML FLA-5-23 strain gages were mounted on the top of each element at 32.5 mm and 62.5 mm locations to measure the longitudinal strains. A strain indicator was adopted to amplify and output the strain readings. The experimental set-up is shown in Fig. 7.

A vertical load of 36.23 N(↓) was applied by hanging a weight 50 mm beyond the end of the beam. It was equivalent to applying a 36.26 N(↓) load and a 1.813 N m (clockwise)

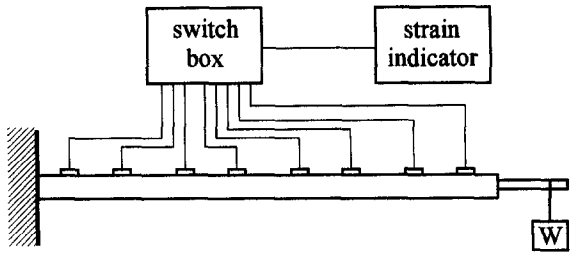


Fig. 7. Experimental set-up.

Table 2. Element strains and identified rigidities of the model test

| Element number | $\varepsilon_1$ ($10^{-6}$) | $\varepsilon_2$ ($10^{-6}$) | $EI$ (N m$^2$) | Error (%) |
|---|---|---|---|---|
| 1 | 605 | 566 | 111.0 | −1.4 |
| 2 | 459 | 422 | 116.2 | 3.2 |
| 3 | 312 | 275 | 116.3 | 3.3 |
| 4 | 165 | 127 | 113.3 | 0.6 |

moment at the end of the beam. The element strains measured in the tests are shown in Table 2.

Substituting these strains into eqn (19) and solving eqn (8), one can obtain the flexural rigidity of each element. The identification took 0.06 s of CPU time. It is seen in Table 2 that the rigidities of the elements have been recovered quite successfully. The errors of the identified rigidities are all below 4%.

## 9. CONCLUSIONS

This paper presents a methodology to identify the flexural rigidity of a beam using the static response of the beam. The finite element analysis is adopted to derive the equilibrium equation of the beam. The identification problem is then formulated as an optimization program in which the error norm of the equilibrium equation is minimized. It is shown that the equilibrium equation can be expressed in terms of the longitudinal strains of the beam elements. Consequently, the element properties can be identified by measuring only element strains in the structural tests. No measurement of nodal displacements or rotations is required. The proposed method is also modified to deal with the situations in which only part of the beam is identified. Both the strain formulation and local identification are important features if the technique is to be applied in practice.

The identifiability of the inverse problem is also addressed in this study. A systematic procedure is introduced to determine how many sets of test data are required to render a unique solution. Following the procedure, useful guidelines on test set-up are derived.

Two numerical examples as well as a model test demonstrate the effectiveness of the proposed method. Several conclusions can be drawn from the examples and the model test. First of all, the identification method can reconstruct the flexural rigidity of a beam successfully. Second, if the finite element model does not represent the physical beam well, as in the tapered beam example, better results can be obtained by applying additional physical constraints on the beam. Third, the error grows as the distance between the element and the load increases. This suggests that the load should be applied in the region of special interest. It also suggests that the ends of the beam are generally not good loading zones. Fourth, the identification results improve as the number of tests increases. Therefore, it is recommended that more tests be carried out in order to obtain more reliable results. Fifth, the method is very efficient. For a 10-element beam, the job takes only 0.08 s of CPU time on a DEC 3000 Model 400 AXP workstation. Sixth, the proposed method is very stable. The coefficients of variation of the identified rigidities only increase linearly with the noise level. This is an indispensable feature for a practical identification method. Finally, the

proposed method can detect the stiffness reduction successfully. Therefore, it can serve as a tool in the non-destructive evaluation of a beam.

*Acknowledgments*—This work was partly supported by the National Science Council of the Republic of China under Grant NSC 82-0115-E-002-389.

## REFERENCES

Agbabian, M. S., Masri, S. F., Miller, R. K. and Caughey, T. K. (1991). System identification approach to detection of structural changes. *J. Engng Mech. ASCE* **117**(2), 370–390.

Berman, A. and Nagy, E. J. (1983). Improvement of a large analytical model using test data. *AIAA J.* **21**(8), 1168–1173.

Baruch, M. and Bar-Itzhack, I. Y. (1978). Optimal weighted orthogonalization of measured modes. *AIAA J.* **16**(4), 346–351.

Chen, J.-C. and Garba, J. A. (1988). On orbit damage assessment for large space structures. *AIAA J.* **26**(9), 1119–1126.

Hajela, P. and Soeiro, F. J. (1990). Structural damage detection based on static and modal analysis. *AIAA J.* **28**(6), 1110–1115.

Hoshiya, M. and Saito, E. (1984). Structural identification by extended Kalman filter. *J. Engng Mech. ASCE* **110**(12), 1757–1770.

Hoshiya, M. and Maruyama, O. (1991). Adaptive identification of autoregressive processes. *J. Engng Mech. ASCE* **117**(7), 1442–1454.

Kabe, A. M. (1985). Stiffness matrix adjustment using mode data. *AIAA J.* **23**(9), 1431–1436.

Kammer, D. C. (1987). Optimum approximation for residual stiffness in linear system identification. *AIAA J.* **26**(1), 104–110.

Lin, C. C., Soong, T. T. and Natke, H. G. (1990). Real-time system identification of degrading structures. *J. Engng Mech. ASCE* **116**(10), 2258–2274.

Liu, P.-L. (1995). Identification and damage detection of trusses using modal data. *J. Structural Engng ASCE* **121**(4), 599–608.

Luenberger, D. G. (1984). *Linear and Nonlinear Programming*. Addison-Wesley, Reading, MA.

Sanayei, M. and Onipede, O. (1991). Damage assessment of structures using static test data. *AIAA J.* **29**(7), 1174–1179.

Sanayei, M. and Scampoli, S. F. (1991). Structural element stiffness identification from static test data. *J. Engng Mech. ASCE* **117**(5), 1021–1036.

Shinozuka, M., Yun, C.-B. and Imai, H. (1982). Identification of linear structural dynamic systems. *J. Engng Mech. ASCE* **108**(6), 1371–1390.

Smith, S. W. and Beattie, C. A. (1991). Secant-method adjustment using mode data. *AIAA J.* **29**(1), 119–126.

Yun, C.-B. and Shinozuka, M. (1980). Identification of nonlinear structural dynamic systems. *J. Structural Mech. ASCE* **8**(2), 187–203.